Formation of evenly spaced ridges and valleys

Formation of evenly spaced ridges and valleys

J. Taylor Perron[1], James W. Kirchner[2,3,4] & William E. Dietrich[2]

[1]Department of Earth, Atmospheric & Planetary Sciences, Massachusetts Institute of Technology, Cambridge, MA 02139, USA. [2]Department of Earth & Planetary Science, University of California, Berkeley, CA 94720, USA. [3]Swiss Federal Institute for Forest, Snow and Landscape Research (WSL), Birmensdorf, Switzerland. [4]Department of Environmental Sciences, Swiss Federal Institute of Technology (ETH), Zürich, Switzerland.

One of the most striking examples of self-organization in landscapes is the emergence of evenly spaced ridges and valleys[1-6]. Despite the prevalence of uniform valley spacing, no theory has been shown to predict this fundamental topographic wavelength. Models of long-term landscape evolution can produce landforms that look realistic[7-9], but few metrics exist to assess the similarity between models and natural landscapes. Here we show that the ridge-valley wavelength can be predicted from erosional mechanics. From equations of mass conservation and sediment transport, we derive a characteristic length scale at which the timescales for erosion by diffusive soil creep and advective stream incision are equal. This length scale is directly proportional to the valley spacing that emerges in a numerical model of landform evolution, and to the measured valley spacing at five field sites. Our results provide a quantitative explanation for one of the most widely observed characteristics of landscapes. They also imply that valley spacing is a fundamental topographic signature that records how material properties and climate regulate erosional processes.

The spacing between adjacent ridges and valleys is a fundamental dimension of hilly topography[1-6]. Even a casual observer can see from an airplane window that ridges

and valleys in many landscapes appear to be uniformly spaced (Fig. 1), even where their locations are not controlled by bedrock structure. Indeed, uniform spacing is often most clearly visible where bedrock is mechanically homogeneous[10]. This implies that the characteristic ridge-valley wavelength is an emergent property of the erosion and sediment transport processes that shape the landscape. Any theory for the long-term evolution of Earth's surface should be able to explain fundamental landscape scales like the ridge-valley wavelength.

Some of the earliest theories of landscape evolution focused on the segmentation of landscapes into ridges (or, more generally, hillslopes) and valleys. Davis[11] and Gilbert[10,12] suggested that hillslopes are dominated by sediment transport mechanisms that smooth the land surface, and that hillslopes give way to valleys where water runoff becomes concentrated enough to outpace the smoothing processes and incise into the land surface. Later studies showed how this competition might lead to the development of evenly spaced valleys. Smith and Bretherton[13] demonstrated that a concave-up, erodible surface under a sheet of flowing water—a situation analogous to a freshly exposed soil embankment during a rainstorm—is unstable with respect to perturbations, with the shortest-wavelength topographic features growing fastest. This result implied no preferred wavelength. Subsequent studies found that if smoothing is introduced, either by diffusive processes[14,15] such as rain splash[16] or by the dispersive effects of the free water surface[2], perturbations with an intermediate wavelength will grow fastest, forming incipient erosional rills with a characteristic spacing. Some studies additionally included a sediment transport threshold that encouraged the selection of an intermediate wavelength[2,5].

These studies considered incipient channelization of a surface by a sheet of flowing water, and cannot be used to predict the dimensions of large-scale landforms like those in Fig. 1. Numerical models based on a similar competition between stream

channel incision and diffusive soil creep have been used to explore the long-term evolution of such landforms, including the factors controlling the upslope drainage area at which hillslopes transition into valleys[8,9,17-21], but not the characteristic ridge-valley wavelength. Moreover, comparisons between models and natural landscapes have been hampered by the scarcity of high-resolution topographic data and the difficulty of measuring the long-term rates of erosion and transport processes in the field.

To investigate the factors that control valley spacing, we developed a numerical model (Methods, Supplementary Information) that simulates landscape evolution under the combined influence of soil creep (here used to mean downslope soil flux due to abiotic and biotic processes that depends linearly on the local surface gradient) and stream incision. The transient evolution of the model illustrates how uniform valley spacing emerges over time (Supplementary Information). As the topography evolves from a randomly rough, horizontal initial surface, irregularly spaced incipient valleys form at the boundaries and begin to grow by lengthening and widening. Competition for drainage area (a proxy for water flux) stunts the growth of valleys that are too small or spaced too closely together. This transient evolution is similar in many respects to early conceptual models of drainage network development[10,16,22]. The model eventually reaches a deterministic equilibrium in which the spacing of valleys is approximately uniform.

Nonlinearities in the governing equation (Equation 1) preclude an analytic solution for the equilibrium topography, so we used dimensional analysis to explore how the erosion and transport parameters control the valley spacing. The governing equation is a nonlinear advection-diffusion equation, and we derived a quantity analogous to a Péclet number, Pe (Equation 2), that expresses the relative magnitudes of the advective stream incision and diffusive soil creep mechanisms shaping the landscape. When Pe is small, the landscape is dominated by creep, and forms a smooth

slope with no valleys. When Pe is large, the landscape is dominated by stream incision, and forms networks of branching valleys. Setting Pe = 1 yields a characteristic length scale, ℓ_c (Equation 3), at which the characteristic timescales for stream incision and creep are equal. Numerical modelling has shown that ℓ_c^2 is approximately the drainage area at which the topography transitions from a concave-down, creep–dominated hillslope to a concave-up, stream incision–dominated valley[23]. We computed equilibrium model solutions using parameters that give a range of values for ℓ_c, and measured valley spacing, λ, by identifying the dominant peaks in the two-dimensional Fourier spectra of the simulated topography[6,23]. For a given value of ℓ_c, a range of valley spacing is possible because a range of slope lengths can give rise to first-order valleys (valleys that do not branch), and longer slopes form more widely spaced valleys (Fig. 2). The range of slope lengths is limited, however, because slopes that are too long will become dissected by branching valleys, and slopes that are too short will remain smooth and undissected. The minimum and maximum valley spacings are directly proportional to ℓ_c, as shown in Fig. 2.

To test whether this theoretical prediction is consistent with valley spacing in natural landscapes, we measured ℓ_c in five landscapes in the United States that have different valley spacings: Gabilan Mesa (GM) and Napa Valley (NV), in the California Coast Ranges; the Dragon's Back pressure ridge (DB) along the San Andreas Fault in the Carrizo Plain, California; Point of the Mountain (PM) in the Salt Lake Valley, Utah; and Eaton Hollow (EH) in southwestern Pennsylvania. All five sites display uniform valley spacing (Fig. 1, Table 1) that is not determined by structural heterogeneities in the underlying bedrock. GM is an oak savannah with a Mediterranean climate, and erosion of the moderately consolidated sandstones, siltstones and conglomerates of the Paso Robles Formation has formed valleys with a spacing of 163 ± 11 m. NV has similar vegetation and climate, with valleys spaced at 128 ± 23 m that have formed in sandstones and mudstones of the Franciscan Complex. DB is a semi-arid grassland

underlain by sediments of the Paso Robles Formation that are less consolidated than in GM, with a valley spacing of 30 ± 3 m. PM is a sand and gravel spit formed by Pleistocene Lake Bonneville, with a valley spacing of 54 ± 13 m. EH is a temperate mixed forest underlain by horizontal beds of Permian and Pennsylvanian sandstone, shale, limestone, and coal, and has a valley spacing of 321 ± 33 m. Valley spacings were measured from peaks in two-dimensional Fourier spectra derived from high-resolution laser altimetry maps[6]. Comparison with spectra for random surfaces with the same roughness characteristics as the observed topography[6] shows that valley spacing as uniform as that observed in the study sites is very unlikely to arise by chance ($p<0.001$).

Erosion and transport at all five sites are dominated by stream channel incision and by diffusive soil creep, which occurs mainly through bioturbation such as tree throw and rodent burrowing. Mean hillslope gradients are between 0.2 and 0.4, and evidence of landslides is rare. In NV, some of the areas surrounding our study site are steeper and have experienced landslides, but we avoided these areas in our analysis. Similarly, portions of DB experience nonlinear creep and frequent landslides due to a spatial gradient in uplift rates[24], but we restricted our analysis to the drainage basins farthest from the zone of maximum uplift, which are dominated by linear creep. The mechanically homogeneous substrates and the two dominant erosion and transport mechanisms conform to the simplifying assumptions behind the numerical model, making these sites suitable locations to test predictions of valley spacing.

An estimate of ℓ_c for each landscape requires values for the constants that describe the long-term strengths of the erosional processes: soil diffusivity D, stream erosivity K, and drainage area exponent m (Equation 3). These parameters are difficult to measure directly because erosion is usually slow or episodic, and because present-day rates may not be representative of long-term rates. We therefore used the shapes of hilltops and

stream profiles measured from high-resolution topography to solve for time-averaged values of D/K and m (Fig. 3, Methods).

The comparison in Fig. 2 shows that valley spacing is proportional to ℓ_c across all five study sites, consistent with the predictions of the numerical model. The good agreement suggests that the two-process model, despite its simplifications, captures the mechanisms that exert the strongest influence on valley spacing in these landscapes. To demonstrate that this agreement is not an inevitable consequence of our procedure for measuring ℓ_c, we performed the same topographic measurements in three landscapes shaped by erosional processes that are not well described by our model; the valley spacing in those landscapes is inconsistent with the inferred values of ℓ_c (Supplementary Information).

Our measurements and the geology and climate of the study sites offer some insight into the differences in ℓ_c and valley spacing. In our model, longer ℓ_c and wider valley spacing can result from larger D, smaller K, or smaller m (Equation 3). Our topographic measurements (Table 1) indicate that the drainage area exponent m is similar for the five sites, and that the differences in valley spacing primarily reflect differences in D/K, the ratio of soil diffusivity to stream erosivity. Systematic variations in bedrock mechanical strength among the five sites further suggest that rock strength, which we expect to be negatively correlated with K, is a major source of variability in D/K. Sites with the least consolidated sediments (DB and PM) have the narrowest valley spacing, sites with moderately consolidated sediments (GM and NV) have intermediate spacing, and the site with the most competent bedrock (EH) has the widest valley spacing.

A comparison of precipitation rates at the five sites (Table 1) suggests that climate may also influence valley spacing: with the exception of GM, wider valley spacing

corresponds to greater present-day mean annual precipitation. One possible cause is the stream erosivity, which depends on drainage basin hydrology as well as on rock strength[7-9,23]. Although higher rainfall should increase streamflow, the dominant effect of precipitation in soil-mantled landscapes like those analysed here may be to reduce K by promoting vegetation growth and infiltration, thereby inhibiting overland flow erosion[9]. It also seems likely that more intense bioturbation in wetter environments leads to higher soil diffusivity[9], an effect consistent with previous measurements[25] of D and with the observed correlation between precipitation and the hilltop curvature, $\nabla^2 z_h$ (Table 1, Methods). Although we are presently unable to quantify the relative importance of these mechanisms, our observations suggest that valley spacing may serve as a topographic proxy for the combined effects of bedrock mechanical strength and climate on the relative magnitudes of different erosional processes.

It is notable that our theory closely predicts valley spacing in the five study sites even though it does not include a threshold for fluvial erosion. Soil cohesion and plant roots impart strength to the soil surface, such that very small flows may not exert enough stress to erode the underlying material. There is evidence that such thresholds influence the locations of fluvial channel heads[26], and it has been proposed that thresholds also influence the scale at which hillslopes transition into valleys[22,27-29]. If a fluvial erosion threshold is included in the model equations, its effect is generally to widen valley spacing[23], though not as much as a comparable fractional change in D or K. The fact that our model does not systematically underpredict valley spacing suggests that competition between soil creep and stream incision is the primary mechanism that controls valley spacing in these landscapes, but we acknowledge that erosion thresholds could have a stronger influence in others.

Also notable is the prediction that ℓ_c, and therefore valley spacing, is independent of erosion rate. This is consistent with previous observations[8,9,23] that steady-state model

topography is independent of erosion rate when both creep flux and stream incision rate vary linearly with topographic slope (Equation 1). The trend in Figure 2, defined by sites that likely have different erosion rates, suggests that this linearity assumption is reasonable.

Valley spacing is a fundamental topographic signature that varies widely across the Earth[1-6,23] and other planetary surfaces[23]. The simplified yet mechanistic approach introduced here enables one to predict valley spacing by parameterizing erosion and transport expressions through topographic analysis. This analysis shows that differences in valley spacing are linked to elementary ratios of rate coefficients that may in turn depend on geologic materials and climate, two regulators of landform evolution that currently are poorly quantified in erosion theory. Thus, valley spacing is a measurable clue to aspects of a site's geologic past that can otherwise be difficult to assess. The same may be true of other emergent patterns in landscapes.

METHODS SUMMARY

Numerical model. Following several previous studies[7-9,17], we describe the evolution of the topography with a nonlinear advection-diffusion equation,

$$\frac{\partial z}{\partial t} = D\nabla^2 z - KA^m|\nabla z| + U \,, \qquad (1)$$

where z is elevation, t is time, D is soil diffusivity, A is drainage area, K and m are constants, and U is surface uplift rate. Equation (1) assumes that soil creep flux is proportional to the local topographic gradient, and that the rate of erosion by channelized flow of water is proportional to the rate of energy expenditure[30]. A derivation of Equation (1) and details of the numerical solution method can be found in ref. 23. Non-dimensionalizing Equation (1) yields a quantity analogous to a Péclet number[23],

$$\mathrm{Pe} = \frac{K\ell^{2m+1}}{D}, \tag{2}$$

where ℓ is a horizontal length scale. Setting Pe = 1, we solved for a characteristic length, ℓ_c, at which the timescales for advection and diffusion are equal,

$$\ell_c = \left(\frac{D}{K}\right)^{\frac{1}{2m+1}}. \tag{3}$$

By solving Equation (1) numerically, we found that the valley spacing, λ, is proportional to ℓ_c (Fig. 2).

Topographic analysis. We used topographic data to infer the value of ℓ_c for the study sites. At equilibrium ($\partial z/\partial t$=0) and on hilltops, where A and ∇z approach zero, Equation (1) reduces to

$$\frac{U}{D} \approx -\nabla^2 z_h, \tag{4}$$

and thus U/D can be inferred from the Laplacian of elevation on hilltops, $\nabla^2 z_h$. Rearranging Equation (1) with $\partial z/\partial t$=0 and using Equation (4) gives

$$\frac{|\nabla z|}{\nabla^2 z - \nabla^2 z_h} = \frac{D}{K} A^{-m}, \tag{5}$$

which implies a power-law relationship between the quantity $|\nabla z|/(\nabla^2 z - \nabla^2 z_h)$, which we abbreviate S^*, and A. We used laser altimetry data to calculate A, $|\nabla z|$, and $\nabla^2 z$, and measured $\nabla^2 z_h$ as the value that $\nabla^2 z$ approaches as $A|\nabla z| \rightarrow 0$ (Fig. 3a). We then calculated S^*, found D/K and m from least-squares regression of $\log_{10}(S^*)$ against $\log_{10}(A)$ (Fig. 3b), and calculated ℓ_c with Equation (3). Values of $\nabla^2 z_h$, D/K, m, ℓ_c, and λ for the five study sites are listed in Table 1.

Supplementary Information is linked to the online version of the paper at www.nature.com/nature.

Acknowledgements This work was supported by the National Science Foundation (J.T.P.), the Institute for Geophysics and Planetary Physics (J.W.K. and J.T.P.), and NASA (W.E.D. and J.T.P.). Laser altimetry for Gabilan Mesa was acquired and processed by the National Center for Airborne Laser Mapping (NCALM, www.ncalm.org) with support from the National Center for Earth-surface Dynamics (NCED). We thank the Orradre family of San Ardo, CA, for granting access to their land, the states of Pennsylvania and Utah for making laser altimetry data publicly available, and Kelin Whipple for his review.

Author Information Correspondence and requests for materials should be addressed to J.T.P. (perron@mit.edu).

1. Shaler, N. S., Spacing of Rivers with Reference to the Hypothesis of Base-levelling. *Geol. Soc. Am. Bull.* **10**, 263-276 (1899).
2. Izumi, N. & Parker, G., Inception of channelization and drainage basin formation: upstream-driven theory. *J. Fluid Mech.* **283**, 341-363 (1995).
3. Hovius, N., Regular spacing of drainage outlets from linear mountain belts. *Basin Res.* **8**, 29-44 (1996).
4. Talling, P. J., Stewart, M. D., Stark, C. P., Gupta, S. & Vincent, S. J., Regular spacing of drainage outlets from linear fault blocks. *Basin Res.* **9**, 275-302 (1997).
5. Izumi, N. & Parker, G., Linear stability analysis of channel inception: downstream-driven theory. *J. Fluid Mech.* **419**, 239-262 (2000).
6. Perron, J. T., Kirchner, J. W. & Dietrich, W. E., Spectral signatures of characteristic spatial scales and non-fractal structure in landscapes. *J. Geophys. Res.* **113**, F04003, doi:10.1029/2007JF000866 (2008).
7. Willgoose, G., Bras, R. L. & Rodriguez-Iturbe, I., Results from a New Model of River Basin Evolution. *Earth Surf. Process. Landf.* **16**, 237-254 (1991).
8. Howard, A. D., A detachment-limited model of drainage basin evolution. *Water Res. Res.* **30**, 2261-2286 (1994).
9. Tucker, G. E. & Bras, R. L., Hillslope processes, drainage density, and landscape morphology. *Water Res. Res.* **34**, 2751-2764 (1998).
10. Gilbert, G. K., *Report on the Geology of the Henry Mountains*. (U.S. Govt. Print. Office, Washington, D. C., 1877).
11. Davis, W. M., The convex profile of badland divides. *Science* **20**, 245 (1892).
12. Gilbert, G. K., The convexity of hilltops. *J. Geol.* **17**, 344-350 (1909).
13. Smith, T. R. & Bretherton, F. P., Stability and the conservation of mass in drainage basin evolution. *Water Res. Res.* **8**, 1506-1529 (1972).

14. Loewenherz, D. S., Stability and the initiation of channelized surface drainage: a reassessment of the short wavelength limit. *J. Geophys. Res.* **96**, 8453-8464 (1991).
15. Simpson, G. & Schlunegger, F., Topographic evolution and morphology of surfaces evolving in response to coupled fluvial and hillslope sediment transport. *J. Geophys. Res.* **108**, 2300, doi:10.1029/2002JB002162 (2003).
16. Dunne, T., Formation and controls of channel networks. *Progress Phys. Geog.* **4**, 211-239 (1980).
17. Kirkby, M. J., Modelling some influences of soil erosion, landslides and valley gradient on drainage density and hollow development. In *Geomorphological Models: Theoretical and Empirical Aspects* (ed. F. Ahnert) 1-14 (*Catena*, Cremlingen-Destedt, 1987).
18. Willgoose, G., Bras, R. L. & Rodriguez-Iturbe, I., A physical explanation of an observed link area-slope relationship. *Water Res. Res.* **27**, 1697-1702 (1991).
19. Tarboton, D. G., Bras, R. L. & Rodriguez-Iturbe, I., A physical basis for drainage density. *Geomorphology* **5**, 59-76 (1992).
20. Howard, A. D., Badland morphology and evolution: Interpretation using a simulation model. *Earth Surf. Process. Landf.* **22**, 211-227 (1997).
21. Moglen, G. E., Eltahir, E. A. B. & Bras, R. L., On the sensitivity of drainage density to climate change. *Water Res. Res.* **34**, 855-862 (1998).
22. Horton, R. E., Erosional development of streams and their drainage basins: hydrophysical approach to quantitative morphology. *Bull. Geol. Soc. Am.* **56**, 275-370 (1945).
23. Perron, J. T., Dietrich, W. E. & Kirchner, J. W., Controls on the spacing of first-order valleys. *J. Geophys. Res.* **113**, F04016, doi:10.1029/2007JF000977 (2008).
24. Hilley, G. E. & Arrowsmith, J. R., Geomorphic response to uplift along the Dragon's Back pressure ridge, Carrizo Plain, California. *Geology* **36**, 367-370 (2008).
25. Fernandes, N. F. & Dietrich, W. E., Hillslope evolution by diffusive processes: The timescale for equilibrium adjustments. *Water Res. Res.* **33**, 1307-1318 (1997).
26. Prosser, I. P. & Dietrich, W. E., Field experiments on erosion by overland flow and their implication for a digital terrain model of channel initiation. *Water Res. Res.* **31**, 2867-2876 (1995).
27. Montgomery, D. R. & Dietrich, W. E., Where do channels begin? *Nature* **336**, 232-234 (1988).
28. Montgomery, D. R. & Dietrich, W. E., Channel initiation and the problem of landscape scale. *Science* **255**, 826-830 (1992).
29. Rinaldo, A., Dietrich, W. E., Rigon, R., Vogel, G. K. & Rodriguez-Iturbe, I., Geomorphological signatures of varying climate. *Nature* **374**, 632-635 (1995).
30. Seidl, M. A. & Dietrich, W. E., The problem of channel erosion into bedrock. In *Functional Geomorphology* (ed. K.H. Schmidt & J. de Ploey) 101-124 (*Catena*, Cremlingen-Destedt, 1992).

Table 1. Topographic measurements

	$\nabla^2 z_h$ ($m^{-1} \times 10^{-3}$)	D/K (m^{2m+1})	m	ℓ_c (m)	λ (m)	Mean ann. precip* (m)
Dragon's Back	-94 ± 3	12 ± 1	0.42 ± 0.01	4.0 ± 0.2	30 ± 3	0.23
Point of the Mountain	-28 ± 4	26 ± 3	0.31 ± 0.02	7.5 ± 0.6	54 ± 13	0.50
Napa Valley	-18.8 ± 0.3	86 ± 13	0.35 ± 0.02	13.7 ± 1.5	128 ± 23	0.93
Gabilan Mesa	-11.8 ± 0.4	124 ± 3	0.35 ± 0.003	17.2 ± 0.4	163 ± 11	0.32
Eaton Hollow	-5.5 ± 0.1	802 ± 82	0.37 ± 0.01	46.0 ± 3.4	321 ± 33	1.05

*For the period 1971-2000. PRISM Group, Oregon State University, http://prismclimate.org.

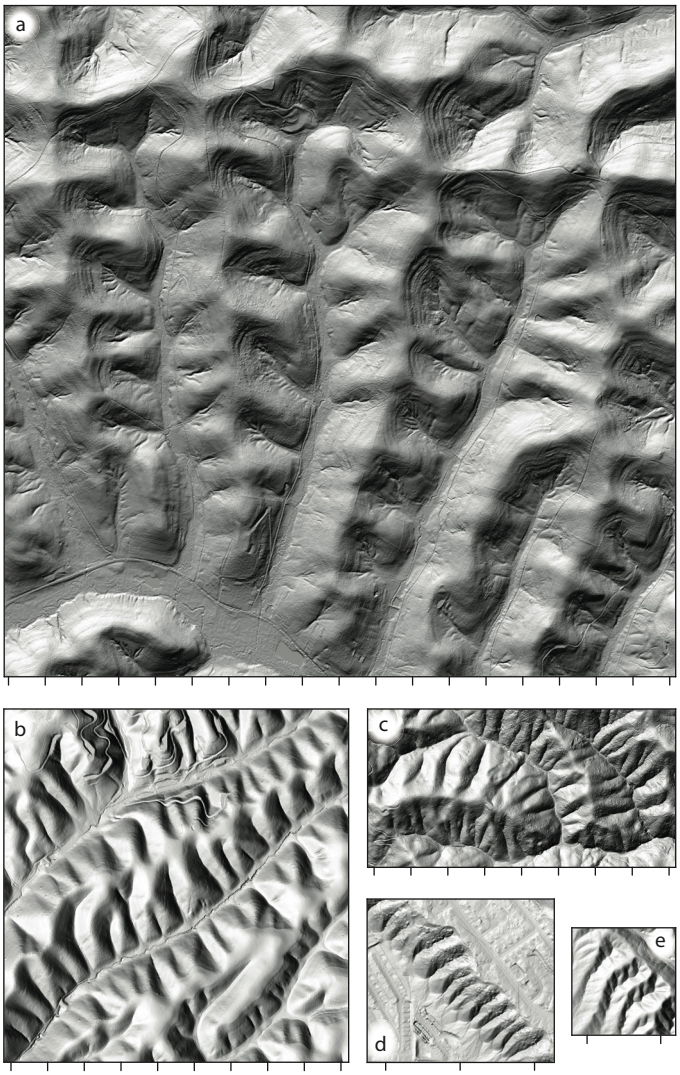

Figure 1. Uniform valley spacing. Shaded relief maps of representative sections of: **a**, Eaton Hollow, Pennsylvania, **b**, Gabilan Mesa, California, **c**, Napa Valley, California, **d**, Point of the Mountain, Utah, **e**, Dragon's Back ridge, California. Tick spacing is 200m. For clarity, **d** and **e** have been enlarged by a factor of 2 relative to **a**-**c**. Vegetation has been filtered out of the data to reveal the underlying topography. Eaton Hollow data are from the State of Pennsylvania PAMAP program; Point of the Mountain data are from the State of Utah Automated Geographic Reference Center; California data are from the National Center for Airborne Laser Mapping (NCALM).

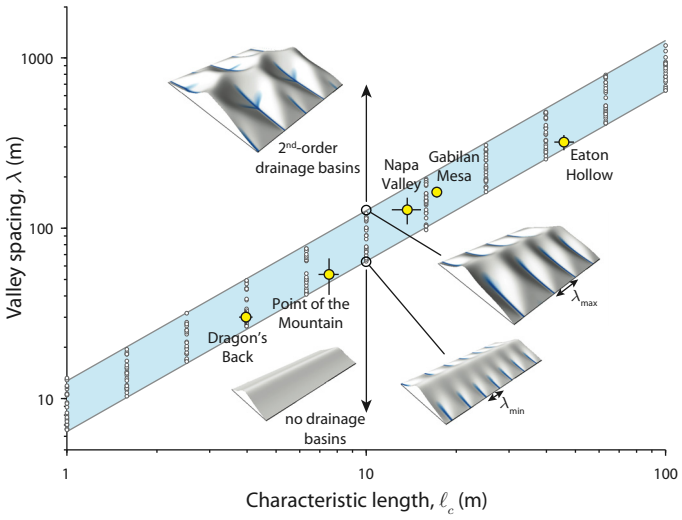

Figure 2. Comparison of predicted and observed valley spacing. Plot of valley spacing, λ, against the characteristic length scale, ℓ_c (Equation 3, Methods), for first-order drainage basins. Each gray circle represents the valley spacing in a single numerical model solution. Blue trend shows the range of possible valley spacings, which correspond to different slope lengths, for each value of ℓ_c. Slope length was controlled by varying the width of the model grid in the direction normal to the main ridgeline. The minimum and maximum spacing for a given value of ℓ_c correspond to the shortest and longest slopes that form first-order valleys. Expression for the blue trend is $6.4\ell_c \leq \lambda \leq 12.7\ell_c$. Insets are perspective views of numerical model solutions with the same ℓ_c but different slope lengths, with valley bottoms shaded blue. Yellow points are the means for first-order valleys in the study sites. Error bars are one standard error of the mean.

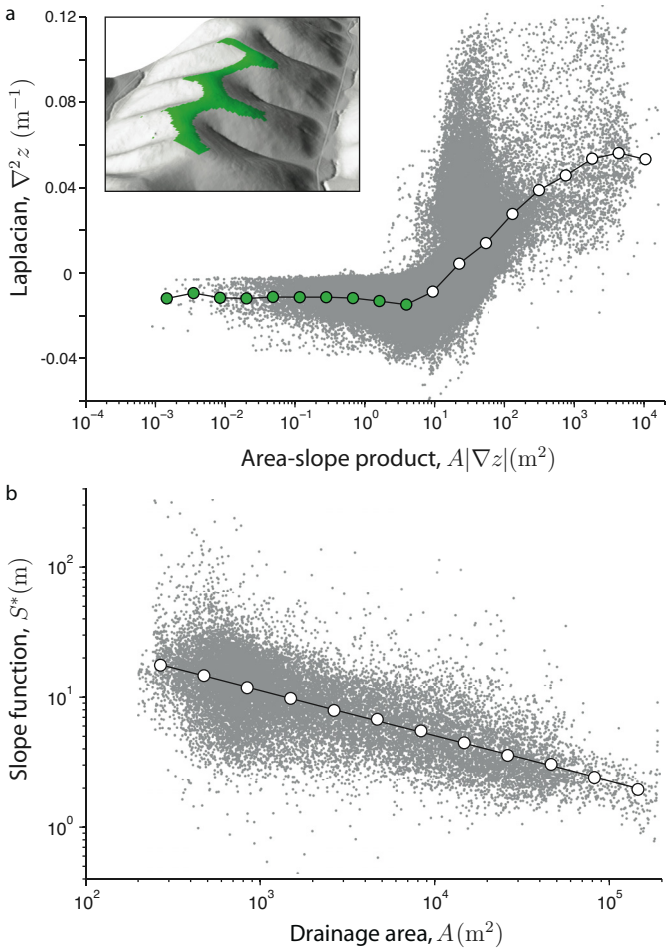

Figure 3. Measurement of model parameters from topography. a, Plot of the Laplacian of elevation against the product of drainage area and slope for first-order drainage basins in Gabilan Mesa. Filled circles are means of log-transformed data within logarithmically spaced bins. On hilltops, where both drainage area and slope are small (green shading), the Laplacian is roughly constant, consistent with equilibrium topography (Equation 4, Methods). Inset shows several representative hilltops. For clarity, the plot shows a random subsample of 25% of the raw data points. **b**, Plot of slope function (Equation 5, Methods) against drainage area for stream profiles in the same basins. Filled circles are means of log-transformed data within logarithmically spaced bins, and line is a least-squares fit to the binned data. Plots for all study sites are shown in the Supplementary Information.

Supplementary Information to accompany "Formation of evenly spaced ridges and valleys"

J. Taylor Perron[1], James W. Kirchner[2,3,4] & William E. Dietrich[2]

[1]Department of Earth, Atmospheric & Planetary Sciences, Massachusetts Institute of Technology, Cambridge, MA 02139, USA. [2]Department of Earth & Planetary Science, University of California, Berkeley, CA 94720, USA. [3]Swiss Federal Institute for Forest, Snow and Landscape Research (WSL), Birmensdorf, Switzerland. [4]Department of Environmental Sciences, Swiss Federal Institute of Technology (ETH), Zürich, Switzerland.

1. Numerical model

1.1. *Supplementary methods*

We solved Equation (1) forward in time on a regular grid with periodic x boundaries and $\nabla^2 z$, ∇z, $U = 0$ at the y boundaries, equivalent to a ridgeline bounded by two streams with constant elevation. The initial condition was a fractal surface with relief approximately 100 times lower than the final surface, and iteration proceeded until $\partial z/\partial t$=0 for all (x,y). Grids ranged from 300×80 to 300×250 points (x×y) with a point spacing of 0.2 to 20 m. Model solutions with the range of ℓ_c shown in Fig. 2 were obtained by varying D and K.

1.2. *Avoiding resolution effects*

Drainage area in landscape evolution models tends to become concentrated in valleys along paths one grid cell wide. If no steps are taken to compensate for this effect, the steady-state topography for a given set of rate parameters can depend on the spatial resolution of the finite difference grid. To prevent the modelled valley spacing from being resolution-dependent, we smoothed the drainage area field with a square moving average kernel at each time step. For filters wider than a few grid points but

narrower than the valleys, valley spacing is only weakly dependent on grid resolution and filter size (Fig. S1). The magnitude of this dependence is comparable to the variability among runs resulting from different initial surfaces. We performed numerical experiments, like that summarized in Fig. S1, to identify the range of acceptable filter sizes for each parameter combination used to construct the blue trend in Fig. 2, and to confirm that the trend is insensitive to spatial resolution. This method for avoiding resolution effects differs from that used in some previous studies of landscape evolution[8,23], but is more broadly applicable.

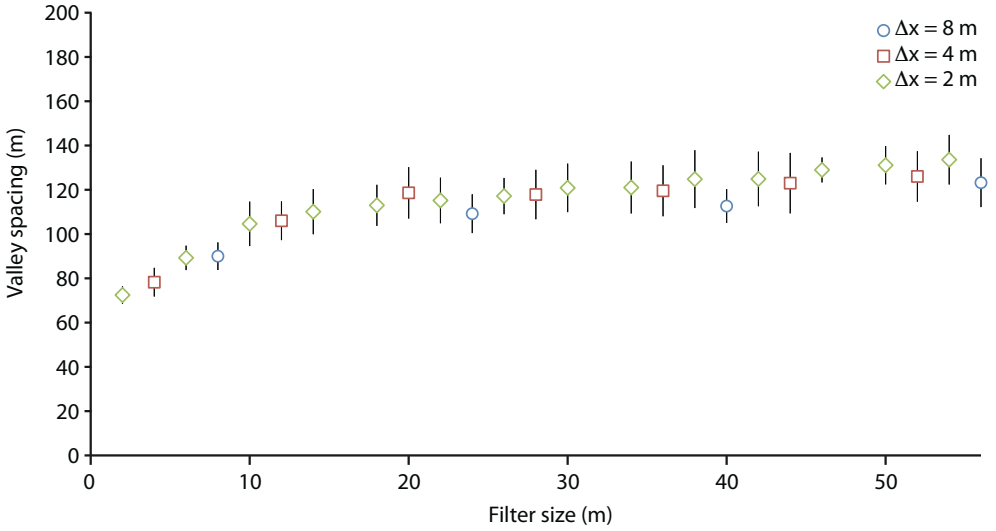

Figure S1. Effects of grid resolution on valley spacing. Plot of modelled valley spacing as a function of drainage area filter size for a range of grid resolutions. Filter sizes correspond to odd numbers of grid points (Δx, $3\Delta x$, $5\Delta x$…). Each point is the mean valley spacing for a set of model runs with ℓ_c = 10.7 m. Error bars are 2σ.

2. Topographic measurements

2.1. *Supplementary methods*

Figure S2 shows the topographic measurements used to calculate ℓ_c for the field sites discussed in the main text. We performed topographic analyses on gridded elevations with a horizontal point spacing of 1 m. We calculated the gradient and Laplacian of elevation from the coefficients of a least-squares quadratic fit to the points

within a 7 m radius. The hilltop Laplacian, $\nabla^2 z_h$, was calculated from the mean values within logarithmically spaced bins over the range of $A|\nabla z|$ for which the binned Laplacian was roughly constant (Fig. 3a).

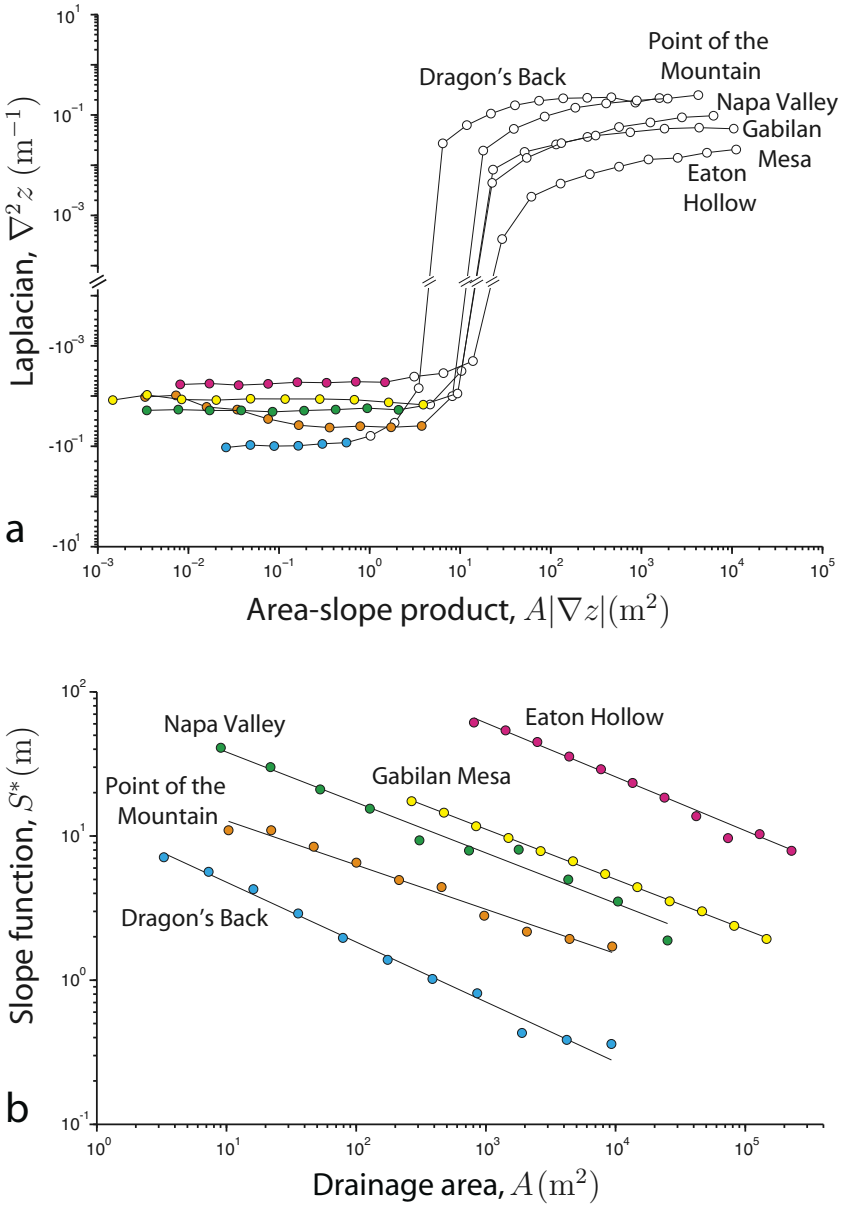

Figure S2. Measurement of model parameters from topography. a, Plot of the Laplacian of elevation against the product of drainage area and slope. Circles are means of log-transformed data within logarithmically spaced bins. Coloured circles are the points used to measure $\nabla^2 z_h$. **b**, Plot of slope function (Equation 5, Methods) against drainage area. Circles are means of log-transformed data within logarithmically spaced bins, and lines are least-squares fits to the binned data.

We mapped the drainage network by starting at a threshold drainage area, which was determined by the square of the wavelength at which a kink in the power spectrum indicated a rapid decline in topographic roughness[6], and then routing flow downslope with a steepest-descent algorithm. Network links with no tributaries were identified as first-order streams. Drainage basins were delineated by starting at the basin outlet, defined as the point just upslope of the junction with a second-order stream, and identifying all upslope points that drain to the outlet. Points showing power-law relationships between S^* and A within individual basins were pooled, and D/K and m were calculated from an iteratively reweighted least-squares fit to the mean values of $\log_{10}(S^*)$ within bins spaced logarithmically in A (Fig. 3b). Uncertainties in ℓ_c were calculated from the uncertainties in D/K, m, and $\nabla^2 z_h$.

2.2. *Test of topographic measurement procedure*

To verify that our method for inferring ℓ_c from high-resolution topographic data can yield a negative result—i.e., a value of ℓ_c that is inconsistent with the relationship between valley spacing and ℓ_c predicted by the numerical model—we applied the measurement procedure to three landscapes shaped by erosional processes that are not well described by the model (Fig. S3). The Zabriskie Point badlands in Death Valley, California, consist of eroded mudstone with a mean valley spacing of 12 ± 3 m, and are completely unvegetated due to highly arid conditions. The steep, nearly planar slopes and sharp drainage divides indicate that hillslope soil transport at Zabriskie Point is dominated by nonlinear creep[31,32], which is not well described by the linear diffusive term in Equation (1). Mettman Ridge in the Oregon Coast Range is a mountainous landscape underlain by sandstone, formerly forested but recently clear-cut, with a valley spacing of 42 ± 12 m. It is a well-documented example of a landscape influenced by nonlinear soil creep[31], with straight slopes and sharp divides similar to those at Zabriskie point. In addition, valley incision in the Oregon Coast Range is known to be strongly influenced by shallow landslides, debris flows[33-37] and, in some locations, deep-seated landslides[38], processes for which no well-documented laws for long-term sediment flux exist, and which therefore are not included in our numerical model. Dark Canyon, which lies within the drainage basin of the south fork of the Eel River in California, is a forested landscape underlain by sandstone and mudstone, and has a

valley spacing of 176 ± 9 m (ref. 6). Like Mettman Ridge, Dark Canyon is steep and experiences both nonlinear soil creep and valley incision by debris flows. Parts of the Eel River basin are strongly affected by deep-seated landslides[39] and earthflows[40]. We therefore do not expect the valley spacing at these three sites to be consistent with the scaling relationship in Fig. 2.

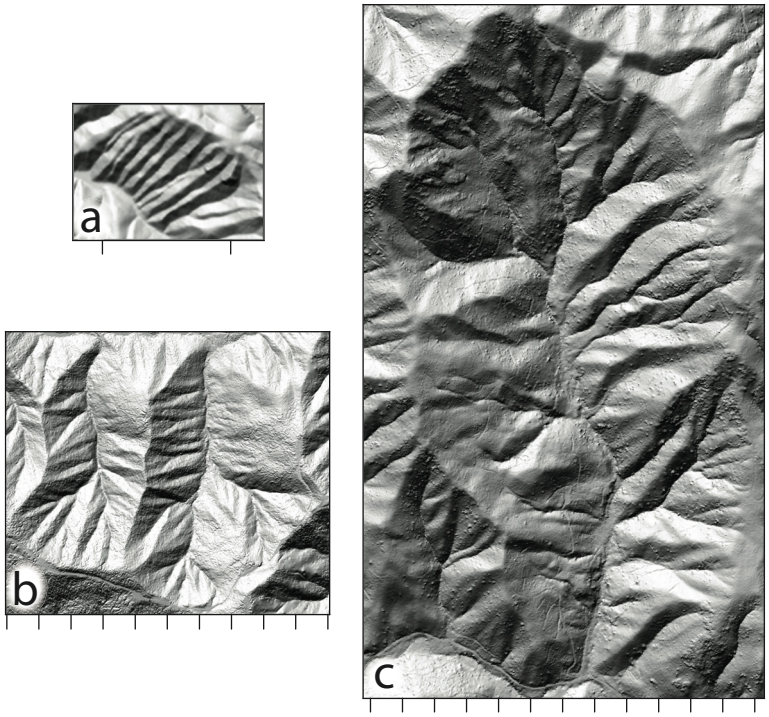

Figure S3. Shaded relief maps of sites with nonlinear soil creep. a, Zabriskie Point, California, **b**, Mettman Ridge, Oregon, **c**, Dark Canyon, California. Tick spacing is 100 m. For clarity, **a** has been enlarged by a factor of 4 relative to **b** and **c**. Laser altimetry data for Zabriskie Point and Dark Canyon are from the National Center for Airborne Laser Mapping (NCALM).

Analysing the topography at Zabriskie Point, Mettman Ridge, and Dark Canyon with the same procedure used for the other study sites, we obtain the values in Table S1. For Zabriskie Point, with $\ell_c = 2.9$ m, the relationship in Fig. 2 predicts a valley spacing between 19 and 37 m, wider than the observed spacing of 12 ± 3 m. The result for Mettman Ridge is similar: for $\ell_c = 9.1$ m, the relationship in Fig. 2 predicts a valley spacing between 59 and 116 m, wider than the observed spacing of 42 ± 12 m. For Dark Canyon, in contrast, the predicted valley spacing of 84 to 166 m for $\ell_c = 13.0$ m is narrower than the observed spacing of 176 ± 9. The overprediction of valley spacing at

Table S1. Topographic measurements for sites with nonlinear creep

	$\nabla^2 z_h$ ($m^{-1} \times 10^{-3}$)	D/K (m^{2m+1})	m	ℓ_c (m)	Observed λ (m)	Predicted λ (m)
Zabriskie Point	-218 ± 19	7 ± 0.4	0.41 ± 0.01	2.9 ± 0.1	12 ± 3	19 – 37
Mettman Ridge	-71 ± 4	26 ± 2	0.24 ± 0.01	9.1 ± 0.7	42 ± 12	59 – 116
Dark Canyon	-30 ± 2	50 ± 3	0.26 ± 0.01	13.0 ± 0.8	176 ± 9	84 – 166

Zabriskie point and Mettman Ridge suggests that valley spacing in landscapes shaped by nonlinear soil creep may be narrower than in landscapes shaped by linear creep. The underprediction at Dark Canyon may be due to the influence of mass wasting processes such as earthflows or deep-seated landslides, which have the demonstrated effect of altering the distribution of topographic variance with respect to wavelength[41]. We conclude from our analysis of these three sites that our method for inferring ℓ_c from topographic data is capable of identifying landscapes that have uniform valley spacing but are inconsistent with the model prediction.

Additional References

31. Roering, J. J., Kirchner, J. W. & Dietrich, W. E., Evidence for nonlinear, diffusive sediment transport on hillslopes and implications for landscape morphology. *Water Res. Res.* **35**, 853-870 (1999).
32. Dietrich, W. E. & Perron, J. T., The search for a topographic signature of life. *Nature* **439**, 411-418 (2006).
33. Dietrich, W. E., Wilson, C. J. & Reneau, S. L., Hollows, colluvium, and landslides in soil-mantled landscapes. In *Hillslope Processes* (ed. A. D. Abrahams) 361-388 (Allen & Unwin, London, 1986).
34. Benda, L., Influence of Debris Flows on Channels and Valley Floors in the Oregon Coast Range, U. S. A. *Earth Surf. Process. Landf.* **15**, 457-466 (1990).
35. Stock, J. & Dietrich, W. E., Valley incision by debris flows: Evidence of a topographic signature. *Water Res. Res.* **39**, 1089, doi:10.1029/2001WR001057 (2003).
36. Stock, J. D., Montgomery, D. R., Collins, B. D., Dietrich, W. E. & Sklar, L., Field measurements of incision rates following bedrock exposure: Implications for process controls on the long profiles of valleys cut by rivers and debris flows. *Geol. Soc. Am. Bull.* **117**, 174-194 (2005).

37. Stock, J. & Dietrich, W., Erosion of steepland valleys by debris flows. *Geol. Soc. Am. Bull.* **118**, 1125-1148 (2006).
38. Roering, J. J., Kirchner, J. W. & Dietrich, W. E., Characterizing structural and lithologic controls on deep-seated landsliding: Implications for topographic relief and landscape evolution in the Oregon Coast Range, USA. *Geol. Soc. Am. Bull.* **117**, 654-668 (2005).
39. Mackey, B. H., Roering, J. J., McKean, J. & Dietrich, W. E., Analyzing the Spatial Pattern of Deep-Seated Landsliding–Evidence for Base Level Control, South Fork Eel River, California. *EOS Trans. AGU* **87**, H53B0619 (2006).
40. Mackey, B. H., Roering, J. J. & McKean, J. A., A Hot Knife Through Ice-Cream: Earthflow Response to Channel Incision (Or Channel Response to Earthflows?), Eel River Canyon, California. *Eos, Trans. AGU* **88**, H43H05 (2007).
41. Booth, A. M., Roering, J. J. & Perron, J. T., Automated landslide mapping using spectral analysis and high-resolution topographic data: Puget Sound lowlands, Washington, and Portland Hills, Oregon. *Geomorphology*, in press (2009).